Ceramics International 46 (2020) 251–257

Contents lists available at ScienceDirect

Ceramics International

journal homepage: www.elsevier.com/locate/ceramint

X-ray photons attenuation characteristics for two tellurite based glass systems at dental diagnostic energies

Y. Al-Hadeethi[a], M.I. Sayyed[b,*], Hiba Mohammed[c,d], Lia Rimondini[c,e]

[a] Department of Physics, Faculty of Science, King Abdulaziz University, Jeddah, 21589, Saudi Arabia
[b] Department of Physics, Faculty of Science, University of Tabuk, Tabuk, Saudi Arabia
[c] Department of Health Sciences, Università del Piemonte Orientale UPO, 28100, Novara, Italy
[d] Fondazione Novara Sviluppo, 28100, Novara, Italy
[e] Interdisciplinary Research Center of Autoimmune Diseases (IRCAD), 28100, Novara, Italy

ARTICLE INFO

Keywords:
X-ray attenuation
Tellurite glasses
WinXcom
Geant4

ABSTRACT

X-ray photons attenuation characteristics for the two tellarite based glasses Bi_2O_3– B_2O_3– TeO_2– TiO_2 and PbO–ZnO–TeO_2–B_2O_3 have been investigated at dental diagnostic energies (between 30-80 keV) using Geant4 code and WinXcom software. The correlation coefficient (R^2) is utilized to evaluate the extent to which Geant4 results are related to the WinXcom data. For the both series, R^2 is close to 1 for all samples and this implies a perfect degree of association between the Geant4 and WinXcom data. The linear attenuation coefficient is proportionally increased with addition of TeO_2 in both series, which implies that there is a decreasing tendency in the X-ray photon transmission corresponding with an increase in the TeO_2 content in the glasses. The half value layer (HVL) decreases as the density increases and this decreasing is very notable at 70 and 80 keV. The maximum HVL for all samples occurs at 80 keV and this implies that the HVL gradually increases as the energy of the X-ray photons increase. Also, the increment of TO_2 in the glasses (in both systems) leads to reduce the mean free path and BiTeTi6 and PbTeB6 samples have the lowest MFP. The MFP for both systems was compared with three heavy concretes and the comparison revealed that the selected systems can be utilized to fabricate protection masks used during diagnostic radiation of the head or oral cavity.

1. Introduction

In dental and medical fields, X-rays are utilized for surgery, radiotherapy and diagnostic treatments. During the diagnostic and therapeutic procedures, the organs and tissues near the area of treatment predominately get exposed to the X-ray photons, causing some damaging or deleterious effects to the living cells or human organism [1–3]. In order to reduce hazards from this type of radiation, radiographers and patients are required to use special protective clothes such as aprons, lead vest, gloves and masks. In practical applications, the lead is the main constituent of these protective materials since it has high density and can completely absorb or attenuate the X-ray photons [4,5]. Generally, lead has noteworthy drawbacks, mainly toxicity and heaviness (the typical lead apron mass is 5–8 kg). Therefore, it is inevitable that medical staffs that use the apron over an extended period of time develop knee and/or back pain. Consequently, a great effort is being made from textile and materials engineers to develop novel non-toxic lead-free protection materials. These alternative materials should have several characteristics such as malleability and ductility, light weight, and highly efficient in attenuation of X-ray photons [6–8]. In order to improve the attenuation capability of the protection materials, heavy chemical elements such as tungsten, antimony, barium and bismuth must be used during the preparation of these materials. On the other hand, radiation masks are used to protect the face from the potential hazards caused by continuing for a long time exposure to X-ray photons during dental and medical treatment. It is not suitable to use an opaque material to synthesize the protection mask and transparent materials are more convenient to be utilized in this regard. Glasses are amorphous materials and can transmit the light and therefore they are promising materials to fabricate the radiation protection mask. Several researchers tried to study and report the interaction between the X-ray photons and some glass systems. Kaewjaeng et al. [9] prepared B_2O_3–CaO– SiO_2–La_2O_3 glass system and studied the x rays shielding for the fabricated glasses. They found that the lead equivalent thickness increases with increasing the La_2O_3 and decreased with the increasing of kilovoltage peak (kVp) of the X-ray machine. Waly et al. [10] utilized

* Corresponding author.
E-mail address: mabualssayed@ut.edu.sa (M.I. Sayyed).

https://doi.org/10.1016/j.ceramint.2019.08.258
Received 14 August 2019; Received in revised form 26 August 2019; Accepted 27 August 2019
Available online 28 August 2019

MicroShield code and reported the photon attenuation factors for different glasses with heavy elements additives between 15 to 300 keV. The authors concluded that the more additives of PbO or Bi_2O_3 to the glass, the superior photon attenuation it provides. The glass with composition 10%SiO_2, 55%Bi_2O_3 and 35% PbO showed the lowest photon exposure rate at low energy (E < 300 keV). MCNPX code helped Almatari et al. [11] to report the attenuation factors for borate based glasses between 20 to 150 keV (medical diagnostic energies) and studied the effect of Li_2O, ZnO and BaO on the attenuating behavior of this system. Their results revealed that the sample with high amount of BaO is suitable in medical fields as X-ray protection material. Tekin et al. [12] investigated the boron phosphate glasses as protection materials in the diagnostic radiology fields. They used Monte Carlo simulation to find the photon attenuation factors for the boron phosphate glasses for energy varying from 60 to 120 keV. The authors compared the photon transmission factor for the boron phosphate glasses with other protection materials to evaluate the potentiality of using this glass system in medical radiation facilities. Hongtong et al. [13] prepared Gd_2O_3–CaF_2–P_2O_5 glass system and studied the X-ray shielding properties using transmission method. The tenth value layer for the samples were found to decrease with increasing Gd_2O_3 content from 5 to 15 mol %, and increased with increasing X-ray energy. The authors also found that this glass system has good X-ray attenuation characteristics at low energy.

Tellurite glasses (based on TeO_2) have distinctive features like low phonon frequency, large transparency window, low melting temperatures, high refractive index and good corrosion resistance [14–18]. Tellurite-based glasses have relatively high density (the density of TeO_2 is 5.67 g/cm^3) and therefore it is expected that those type of glasses can effectively diminish the effect of the radiation.

In this work, two tellurite based glasses namely Bi_2O_3– B_2O_3– TeO_2– TiO_2 (BiTeTi1– BiTeTi6 glasses) and PbO–ZnO–TeO_2–B_2O_3 (PbTeB1– PbTeB6 glasses) were selected, and their capability to shield diagnostic X-ray photons (between 30-80 keV) were investigated. We used Geant4 for evaluation the attenuation parameters for the two investigated glasses and then we compared the results with the other commonly used materials for radiation shielding aims.

2. Materials and method

X-ray photons attenuation characteristics for the two tellurite based glasses namely Bi_2O_3– B_2O_3– TeO_2– TiO_2 (coded as BiTeTi1– BiTeTi6 glasses) and PbO–ZnO–TeO_2–B_2O_3 (coded as PbTeB1– PbTeB6 glasses) have been investigated in this work at dental diagnostic energies (between 30-80 keV). The elemental composition of the BiTeTi1– BiTeTi6 glasses whose densities varying from 4.67 to 5.95 g/cm^3 and PbTeB1– PbTeB6 glasses whose varying ranging from 4.58 to 6.52 g/cm^3 are summarized in Table 1 and Table 2 [19,20]. To achieve the aim of this work, we evaluated the X-ray attenuation parameters for the selected glass systems and then compared the results with the other commonly used materials for radiation sheilding. In this section we will discuss in brief the photon attenuation parameters.

If X-ray photons pass through attenuator (glass specimen in our work), part of the photons is attenuated by the attenuator and the residual photons cross the attenuator. Beer-Lambert law is suitable relation used to describe the attenuation occurred for the photons [12]:

$$I = I_0 e^{-\mu x} \tag{1}$$

The previous relation gives an indication of the attenuation capacity of the material. The term μ is called the linear attenuation coefficient that estimates how a photon with specific energy will be attenuated when moving through the glass sample [21]. μ for any attenuator depends on the density of the attenuator, the energy of the photons and the chemical composition of the attenuator.

The mass attenuation coefficient (μ/ρ) is also a useful quantity to evaluate the capability of a medium to shield the photons. For a sample consists of different elements (such as O, B, Te, Ti and Bi in the first glass system), the mixture rule is convenient way to determine the μ/ρ at any energy [11]:

$$\mu/\rho = \sum_i w_i (\mu/\rho)_i \tag{2}$$

where w_i is the weight fraction for the elements (given in Table 1 for BiTeTi1– BiTeTi6 glasses, and in Table 2 for PbTeB1– PbTeB6 glasses). The μ/ρ values for the elements at the investigated energies (dental diagnostic energies 30 < E < 80 keV) were taken from WinXcom software [22]. Also, the μ/ρ for the glasses under study was estimated by Geant4 simulation code [23]. It is worth mentioning that high values of the previous two parameters indicate the good attenuation capabilities of the medium.

Half-value layer (HVL) practically measures the thickness of the attenuator needed to diminish the photons intensity to 50% of its initial value. This parameter reflects the thickness of the glass sample that can replace the protective garments incorporating lead (Pb)/or lead masks during diagnostic radiation of the head or oral cavity. Mathematically, HVL is expressed as in the next formula [24]:

$$HVL = \frac{0.693}{\mu} \tag{3}$$

Generally, to provide an efficient photons shielding, the glass sample must contain heavy elements so the photons can interact easily with the atoms. In our two glass systems, the TeO_2, Bi_2O_3 and PbO are helpful in attenuating the incident photons.

The mean free path (MFP) is a density dependent parameter and represents the reciprocal of μ [25]:

$$MFP = \frac{1}{\mu} \tag{4}$$

3. Results and discussion

Geant4 simulation results of μ/ρ for the BiTeTi1– BiTeTi6 glasses and PbTeB1– PbTeB6 glasses at dental diagnostic energies (between 30-80 keV) and WinXcom results are summarized in Tables 3 and 4 respectively. Also, we plotted the μ/ρ (Geant4 and WinXcom data) for BiTeTi1 and PbTeB1 (as an example from the first and second series) in Fig. 1 and Fig. 2. It is evident that the Geant4 results are matching with the calculated values. The correlation coefficient (R^2) which estimates the linear association between two variables is used to evaluate the extent to which Geant4 results are related to the WinXcom data. For

Table 1
The chemical composition and the density of the Bi_2O_3– B_2O_3– TeO_2– TiO_2 glass series.

Density (g/cm^3)	Bi	Te	Ti	O	B	TiO_2	TeO_2	B_2O_3	Bi_2O_3	Glass code
4.67	0.43903	0.30157	0.02515	0.20587	0.02839	10	45	25	20	BiTeTi1
5.00	0.43538	0.31236	0.01995	0.20416	0.02815	8	47	25	20	BiTeTi2
5.11	0.43179	0.32297	0.01484	0.20248	0.02792	6	49	25	20	BiTeTi3
5.53	0.42827	0.33340	0.00981	0.20083	0.02769	4	51	25	20	BiTeTi4
5.72	0.42479	0.34367	0.00487	0.19919	0.02747	2	53	25	20	BiTeTi5
5.95	0.42138	0.35377	0	0.19759	0.02725	0	55	25	20	BiTeTi6

Table 2
The chemical composition and the density of the PbO–ZnO–TeO_2–B_2O_3 glass series.

Density (g/cm^3)	Pb	Te	Zn	O	B	B_2O_3	TeO_2	ZnO	PbO	Glass code
4.58	0.37103	0.11425	0.11709	0.30083	0.09679	50	10	20	20	PbTeB1
5.22	0.31955	0.29518	0.10085	0.23441	0.05002	30	30	20	20	PbTeB2
5.53	0.29882	0.36804	0.09430	0.20766	0.03118	20	40	20	20	PbTeB3
5.87	0.28062	0.43202	0.08856	0.18418	0.01464	10	50	20	20	PbTeB4
6.22	0.38404	0.39417	0.04039	0.16804	0.01336	10	50	10	30	PbTeB5
6.52	0.36381	0.44809	0.03827	0.14983	0	0	60	10	30	PbTeB6

Table 3
The mass attenuation coefficients (cm^2/g) of the Bi_2O_3– B_2O_3– TeO_2– TiO_2 glasses using Geant4 code and WinXcom software.

Mass attenuation coefficients (cm^2/g)												Energy (keV)
BiTeTi6		BiTeTi5		BiTeTi4		BiTeTi3		BiTeTi2		BiTeTi1		
WinXcom	Geant4	WinXcom	Geant4	WinXcom	Geant4	WinXcom	Geant4	WinXcom	Geant4	WinXcom	Geant4	
16.150	15.234	16.200	15.288	16.250	15.343	16.310	15.398	16.360	15.455	16.420	15.512	30
13.660	13.017	13.510	12.871	13.370	12.723	13.210	12.572	13.060	12.419	12.900	12.263	40
7.628	7.154	7.547	7.074	7.465	6.993	7.381	6.910	7.297	6.826	7.210	6.741	50
4.738	4.382	4.689	4.334	4.639	4.285	4.588	4.234	4.536	4.184	4.484	4.132	60
3.173	2.903	3.141	2.871	3.108	2.839	3.075	2.807	3.042	2.774	3.007	2.740	70
2.251	2.040	2.229	2.018	2.207	1.996	2.184	1.974	2.161	1.951	2.138	1.928	80

Table 4
The mass attenuation coefficients (cm^2/g) of the PbO–ZnO–TeO_2–B_2O_3 glasses using Geant4 code and WinXcom software.

Mass attenuation coefficients (cm^2/g)												Energy (keV)
PbTeB6		PbTeB5		PbTeB4		PbTeB3		PbTeB2		PbTeB1		
WinXcom	Geant4	WinXcom	Geant4	WinXcom	Geant4	WinXcom	Geant4	WinXcom	Geant4	WinXcom	Geant4	
15.080	14.115	15.300	14.344	13.050	12.211	13.180	12.354	13.330	12.518	13.700	12.924	30
14.720	14.069	13.920	13.268	13.480	12.911	12.460	11.900	11.300	10.750	8.412	7.892	40
8.199	7.728	7.756	7.290	7.501	7.092	6.939	6.539	6.299	5.909	4.711	4.346	50
5.077	4.726	4.808	4.462	4.643	4.338	4.302	4.004	3.912	3.624	2.946	2.680	60
3.389	3.123	3.214	2.952	3.100	2.868	2.877	2.652	2.623	2.405	1.993	1.793	70
2.396	2.188	2.276	2.071	2.192	2.011	2.039	1.863	1.865	1.694	1.432	1.275	80

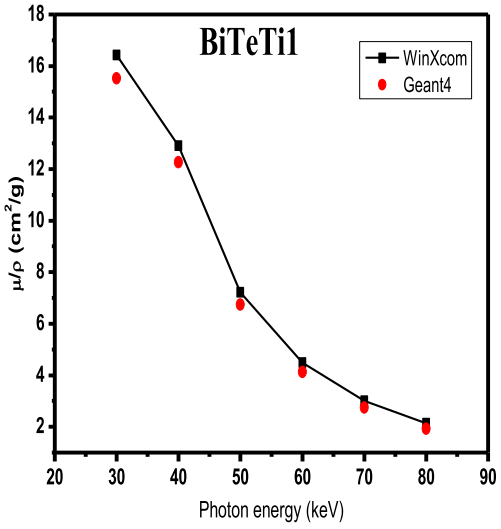

Fig. 1. Comparison between the mass attenuation coefficients (cm2/g) of the BiTeTi1 glass using Geant4 code and WinXcom.

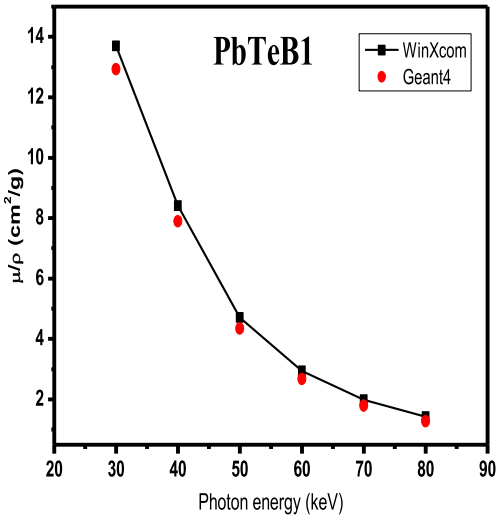

Fig. 2. Comparison between the mass attenuation coefficients (cm2/g) of the PbTeB1 glass using Geant4 code and WinXcom.

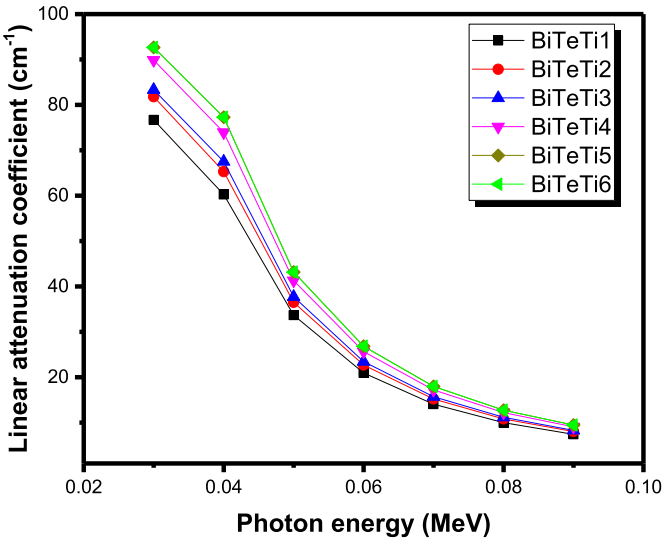

Fig. 3. The linear attenuation coefficient for Bi2O3– B2O3– TeO2– TiO2 glass system between 30 keV to 90 keV.

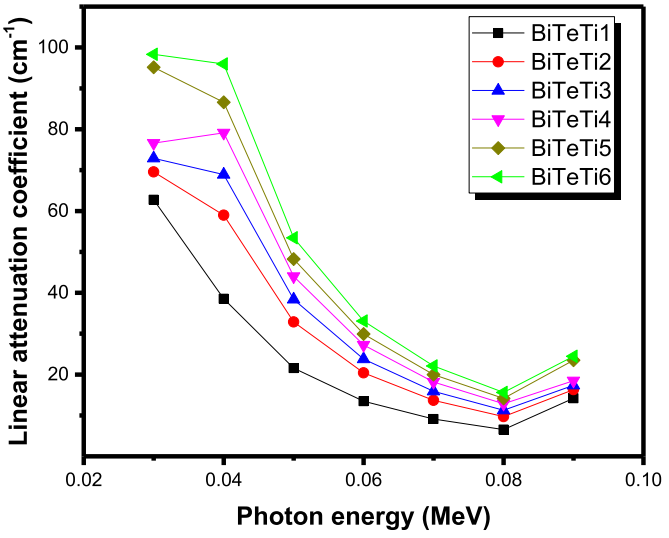

Fig. 4. The linear attenuation coefficient for PbO–ZnO–TeO2–B2O3 glass system between 30 keV to 90 keV.

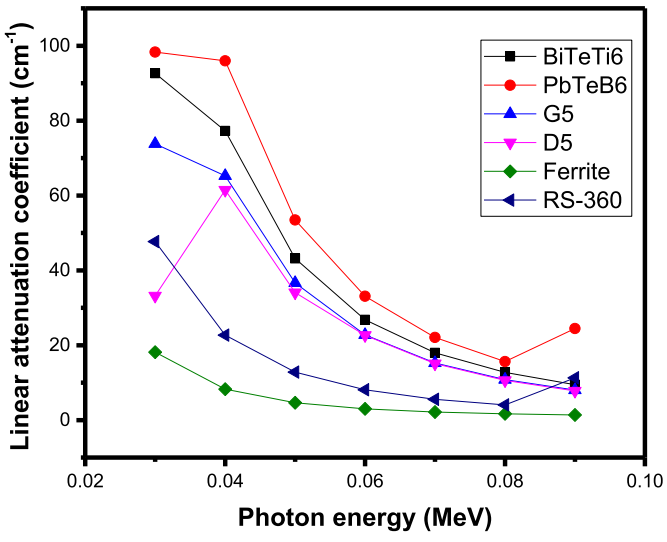

Fig. 5. Chart of linear attenuation coefficients of BiTeTi6 and PbTeB6 samples and other commonly used materials for shielding.

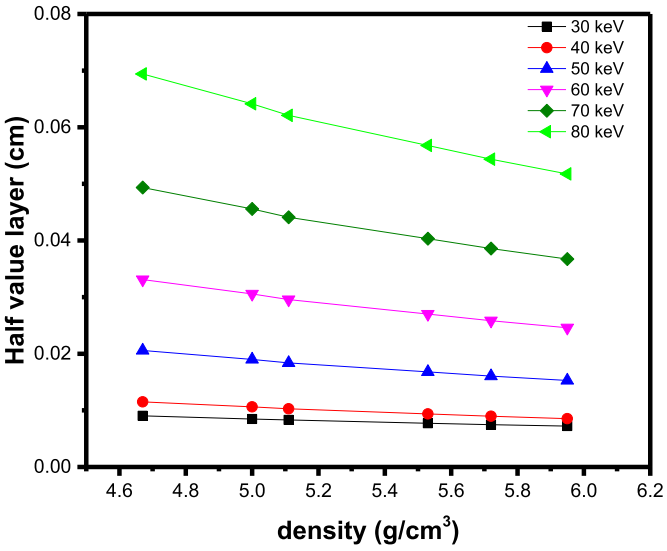

Fig. 6. The variation of half value layer (cm) with the density for Bi2O3–B2O3– TeO2– TiO2 glass system.

both series, R^2 is close to 1 for all samples and this implies a perfect degree of association between the Geant4 and WinXcom data.

Fig. 3 and Fig. 4 present the μ results of the BiTeTi1– BiTeTi6 glasses and PbTeB1– PbTeB6 glasses respectively. From the curves, the μ is proportionally increased with the addition of TeO_2 (from 45 to 55 mol% in the first series and from 10 to 60 mol% in the second one). This is attributed to the increase of the sample density with increasing TeO_2 content and it is known that the μ is depends directly upon the density of the medium. For example, due to increase in the density from 4.67 to 5.95 g/cm^3 in the first series, the μ increased from 76.68 to 96.09 cm^{-1} at 30 keV. Similarly, the μ increased from 62.75 to 98.32 cm^{-1} at the same energy (i.e.30 keV) due to the increase in the density for the samples in the second series from 4.58 to 6.52 g/cm^3. This finding implies that there is a decreasing tendency in the X-ray photon transmission corresponding with an increase in the TeO_2 content in the glasses (or increase the density). Accordingly, the selected tellurite based glasses shielding capability has been increased by the addition of TeO_2. Therefore, we can state that the high density glass specimen can effectively absorb the X-ray and used as an alternative protective mask during diagnostic radiation of the head or oral cavity.

It is evident from Figs. 3 and Fig.4 that the energy is another factor affecting the X-ray attenuation for the glasses. Firstly, the μ is high which means that the magnitude of attenuation is very high and this is attributed to predominant of the photoelectric effect. This process depends extremely on the atomic number and the Te, Pb and Bi elements have a significant contribution on this process at low energy, so we noticed the high μ values for low energy.

Moreover, in Fig. 5, the μ of BiTeTi6 and PbTeB6 glasses when compared with four ordinarily utilized protection materials showed some promising outcomes. As BiTeTi6 and PbTeB6 glasses have the highest μ values in series one and two, so we selected these two samples and compared them with barium–Bismuth–Borosilicate glass (G5) [26], erbium zinc tellurite glass (D5) [27], RS-360 glass (contains 45 mol% of PbO) [28] and Ferrite concrete [29]. It is clear that PbTeB6 has higher μ than BiTeTi6 and the both samples have higher μ than the materials used for the sake of comparison. Hence, the selected tellurite based glasses are more effective shielding materials.

Figs. 6 and 7 show the relationship between HVL and sample density of Bi_2O_3– B_2O_3– TeO_2– TiO_2 and PbO–ZnO–TeO_2–B_2O_3 glass systems between 30 and 80 keV. These two figures show that the HVL

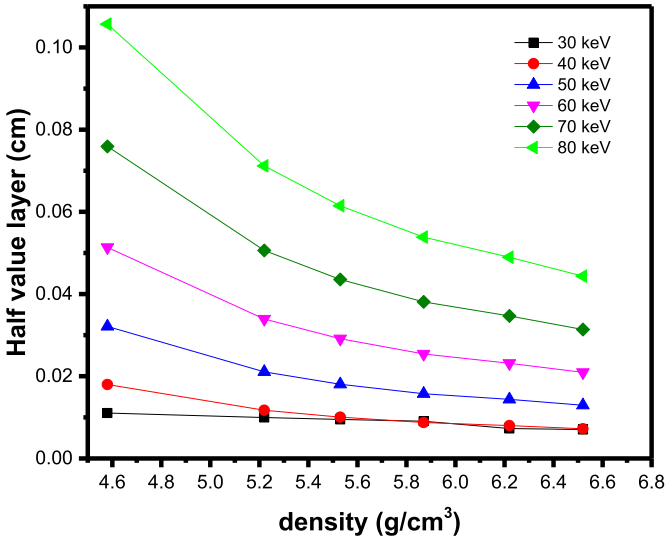

Fig. 7. The variation of half value layer (cm) with the density for PbO–ZnO–TeO2–B2O3 glass system.

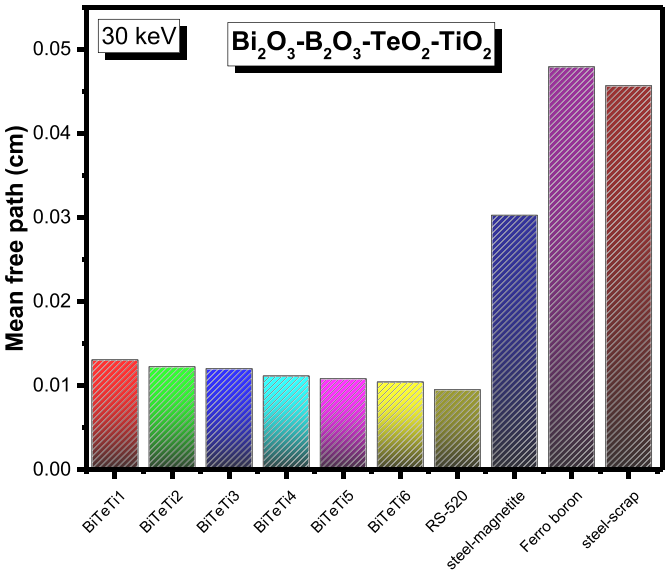

Fig. 8. Comparison between the mean free path (cm) for Bi2O3– B2O3– TeO2–TiO2 glass system with some nuclear engineering materials at 30 keV.

decreases as the density increases and this decreasing in HVL is very notable at 70 and 80 keV. The heavier the glass sample, the lower is the value of HVL and can be used as effective x-ray protection materials. As expected, the HVL depends highly on the density of the specimen and hence this parameter can satisfactorily characterize the influence of TeO_2 content on the attenuation capability of the tellurite glasses against X-rays. The heavy elements in the glasses (Te, Pb and Bi) present larger target for the X-ray photons to strike and therefore the likelihoods of interactions are comparatively high and increased with the more amount of TeO_2. So, the attenuation should be comparatively high and the X-rays photons have less probability of being transmitted through the high density glass sample. This fact explains the low HVL value for the two samples BiTeTi6 ($\rho = 5.95\ g/cm^3$) and PbTeB6 ($\rho = 6.52\ g/cm^3$). This finding is in agreement with that of Agar et al. [30], in which the HVL for P_2O_5, BaO and MoO_3 glasses decrease with increasing the density. The same conclusion was reported by Ersundu et al. [31].

Also, from Figs. 6 and Fig.7 we can see that the maximum HVL for all glasses takes place at 80 keV. This implies that the HVL gradually

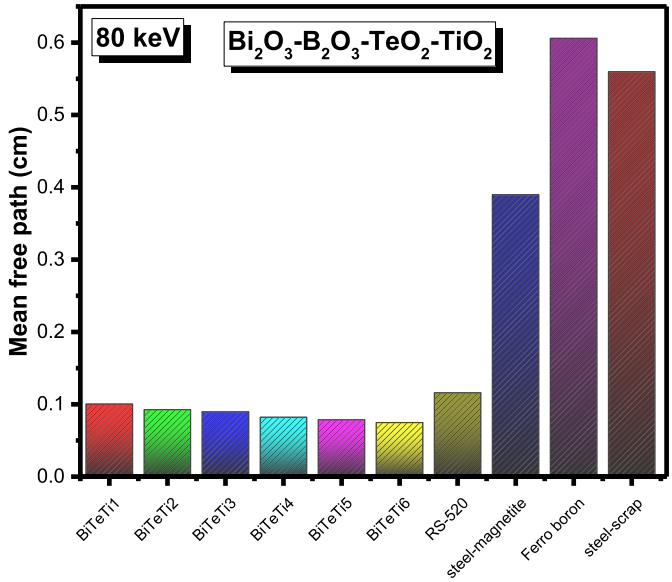

Fig. 9. Comparison between the mean free path (cm) for Bi2O3– B2O3– TeO2–TiO2 glass system with some nuclear engineering materials at 80 keV.

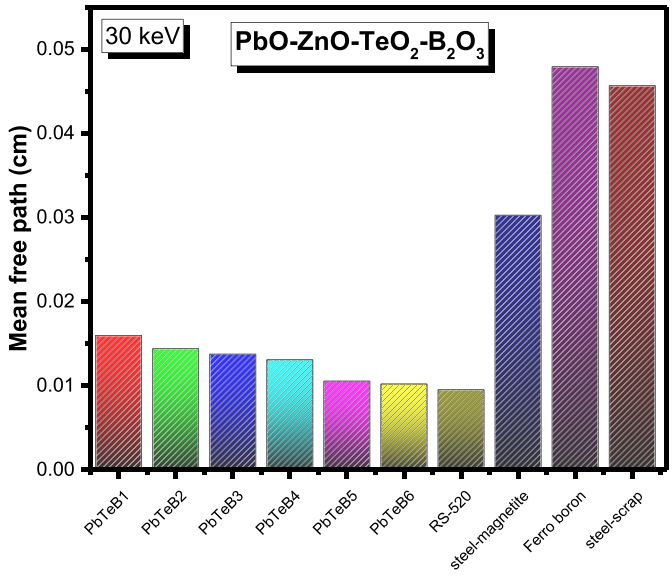

Fig. 10. Comparison between the mean free path (cm) for PbO–ZnO–TeO2–B2O3 glass system with some nuclear engineering materials at 30 keV.

increases as the energy of the X-ray photons increases. With the increment of the X-rays energy from 30 to 80 keV, the HVL of BiTeTi6 increased from 0.0072 to 0.1023 cm, and for PbTeB6 it increased from 0.0070 to 0.1009 cm. The present dependence of HVL on the energy suggests that the penetrating power of X-ray photons significantly increases with increasing the energy of the photons. It can be also noticed from Fig.6 and Fig. 7 that the HVL changes slightly at 30 and 40 keV. This suggests that it is preferable to increase the thickness of the specimen for the applications which require high X-rays photons ($E > 40$ keV).

In Fig. 8 and Fig. 9 we plot the MFP of the Bi_2O_3– B_2O_3– TeO_2– TiO_2 glass system in comparison with some nuclear engineering materials at 30 keV and 80 keV respectively. The nuclear engineering materials used for the sake of comparison are one commercial glass contains 71 mol% of lead (coded as RS-520, with density = $5.2\ g/cm^3$) [32], three high density concretes namely ferro boron concrete (contains 72% Fe with

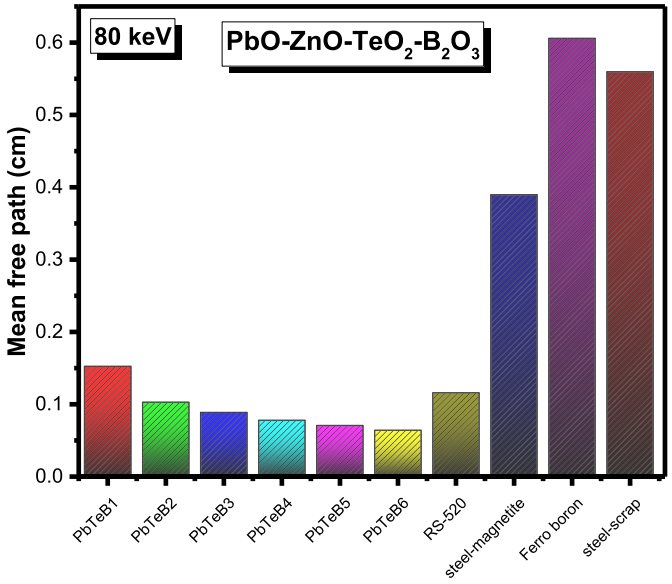

Fig. 11. Comparison between the mean free path (cm) for PbO–ZnO–TeO2–B2O3glass system with some nuclear engineering materials at 80 keV.

density = 3.5 g/cm^3) [33], steel magnetite (contains 75.73% Fe, with density = 5.11 g/cm^3) and steel-scrap (contains 61.25% Fe, with density = 4 g/cm^3) [34]. In Fig. 10 and Fig. 11 we plot the MFP of the PbO–ZnO–TeO_2–B_2O_3 glasses in comparison with the aforementioned nuclear engineering materials at 30 keV and 80 keV respectively.

From these figures, it is noticed that the increment of TO_2 in the glasses (in both systems) leads to a decrease in MFP at 30 and 80 keV (this is also true for 40, 50, 60 and 70 keV but we didn't show the results). BiTeTi6 and PbTeB6 have the lowest MFP among the samples under investigation and this is in agreement with the HVL results. This is because TeO_2 increases the density which is related to μ of the samples and MFP is the reciprocal of μ. From Figs. 8 and Fig.9 we can observe that the three heavy concretes have higher MFP than BiTeTi1–BiTeTi6 glasses indicating that the Bi_2O_3– B_2O_3– TeO_2– TiO_2 glass system can be used as protection glasses at dental diagnostic energies. The results show that the MFP of BiTeTi6 is comparable with RS-520 at 30 keV and slightly lower than RS-520 at 80 keV. In Figs. 10 and Fig.11 also the results show that the MFP of PbO–ZnO–TeO_2–B_2O_3 glasses are lower than steel magnetite, ferro boron and steel-scrap concretes at 30 and 80 keV, while RS-520 has comparable MFP with PbTeB6 at 30 keV.

4. Conclusion

The X-ray attenuation properties of BiTeTi1– BiTeTi6 and PbTeB1–PbTeB6 glasses have been reported. The simulated μ/ρ was validated by a comparison with the results obtained by WinXcom. The correlation coefficient (R^2) is used to evaluate the extent to which Geant4 results are related to the WinXcom data. The μ is proportionally increased with the addition of TeO_2 in both series, which implies that there is a decreasing tendency in the X-ray photon transmission corresponding with an increase in the density of the samples. The HVL reduces as the density increases especially at 70 and 80 keV. The maximum HVL for all samples occurs at 80 keV and this suggested that the HVL increases as the energy of the X-ray photons increase. Furthermore, the increment of TO_2 in the both systems leads to a decrease in MFP at all energies and BiTeTi6 and PbTeB6 samples have the lowest MFP. We compared the MFP of both systems with steel magnetite, ferro boron and steel-scrap concretes and the comparison revealed that the selected glasses can be utilized to fabricate protection masks used during diagnostic radiation of the head or oral cavity.

Acknowledgment

This project was funded by the Deanship of Scientific Research, King Abdulaziz University, Jeddah, under grant No. (D-291-130-1440). The authors, therefore, gratefully acknowledge the DSR technical and financial support.

References

[1] Anil Kumar Singh, Rakesh Kumar Singh, Bhupesh Sharma, Ajay Kumar Tyagi, Characterization and biocompatibility studies of lead free X-ray shielding polymer composite for healthcare application, Radiat. Phys. Chem. 138 (2017) 9–15.
[2] Mengge Dong, Xiangxin Xu, Shan Liu, Yang He, Zhefu Li, M.I. Sayyed, O. Agar, Using iron concentrate in Liaoning Province, China, to prepare material for X-Ray shielding, J. Clean. Prod. 210 (2019) 653e659.
[3] Karoline Günther, Christina Giebing, Antonia Askani, Tilmann Leisegang, Marcus Krieg, Yordan Kyosev, Thomas Weide, Boris Mahltig, Cellulose/inorganic-composite fibers for producing textile fabrics of high X-ray absorption properties, Mater. Chem. Phys. 167 (2015) 125–135.
[4] M.R. Kaçal, F. Akman, M.I. Sayyed, F. Akman, Evaluation of gamma-ray and neutron attenuation properties of some polymers, Nucl. Eng. Technol. 51 (2019) 818–824.
[5] Ji Woo Hong, Dae Ho Kim, Seok Won Kim, Seong Hoon Choi, Ga-Eul Lee, Hyun-Kyu Seo, Sang-Hyun Kim, Youngjin Lee, Effectiveness evaluation of self-produced micro- and nanosized tungsten materials for radiation shielding with diagnostic X-ray imaging system, Optik - Int. J. Light Electron Opt. 172 (2018) 760–765.
[6] F. Akman, I.H. Geçibesler, A. Kumar, M.I. Sayyed, M.H.M. Zaid, Evaluation of radiation absorption characteristics in different parts of some medicinal aromatic plants in the low energy region, Res. Phys. 12 (2019) 94–100.
[7] Munirah Jamil, Muhammad Hazritz Hazlan, Ramzun Maizan Ramli, Nurul Zahirah Noor Azman, Study of electrospun PVA-based concentrations nanofibre filled with Bi2O3 or WO3 as potential x-ray shielding material, Radiat. Phys. Chem. 156 (2019) 272–282.
[8] N.Z. Noor Azman, N.F.L. Musa, N.N.A. Nik Ab Razak, R.M. Ramli, I.S. Mustafa, A. Abdul Rahman, N.Z. Yahaya, Effect of Bi2O3 particle sizes and addition of starch into Bi2O3–PVA composites for X-ray shielding, Appl. Phys. A 122 (2016).
[9] S. Kaewjaeng, S. Kothan, W. Chaiphaksa, N. Chanthima, R. Rajaramakrishna, H.J. Kim, J. Kaewkhao, High transparency La2O3-CaO-B2O3-SiO2 glass for diagnosis x-rays shielding material application, Radiat. Phys. Chem. 160 (2019) 41–47.
[10] El-Sayed A. Waly, Ghada Shkoukani Al-Qous, Mohamed A. Bourham, Shielding properties of glasses with different heavy elements additives for radiation shielding in the energy range 15–300 keV, Radiat. Phys. Chem. 150 (2018) 120–124.
[11] M. Almatari, O. Agar, E.E. Altunsoy, O. Kilicoglu, M.I. Sayyed, H.O. Tekin, Photon and neutron shielding characteristics of samarium doped lead alumino borate glasses containing barium, lithium and zinc oxides determined at medical diagnostic energies, Results Phys. 12 (2019) 2123–2128.
[12] H.O. Tekin, E.E. Altunsoy, E. Kavaz, M.I. Sayyed, O. Agar, M. Kamislioglu, Photon and neutron shielding performance of boron phosphate glasses for diagnostic radiology facilities, Res. Phys. 12 (2019) 1457–1464.
[13] W. Hongtong, S. Kaewjaeng, S. Kothan, P. Meejitpaisan, W. Cheewasukhanont, P. Limkitjaroenporn, J. Kaewkhao, Development of gadolinium doped calcium phosphate oxyfluoride glasses for X-ray shielding materials, Mater. Today: Proc. 5 (2018) 14063–14068.
[14] Helena Ticha, Jiri Schwarz, Ladislav Tichy, Raman spectra and optical band gap in some PbO-ZnO-TeO2 glasses, Mater. Chem. Phys. 237 (2019) 121834.
[15] N. Gedikoğlu, A.E. Ersundu, S. Aydin, M. Çelikbilek Ersundu, Crystallization behavior of WO3-MoO3-TeO2 glasses, J. Non-Cryst. Solids 501 (2018) 93–100.
[16] Kyong-Soo Hong, Miae Kim, Myoung Gyu Ha, Jong Pil Kim, Jang-Hee Yoon, Jong Hwa Kim, Ho-Soon Yang, Hyun Gyu Kim, Red-emission properties and crystallization behavior in Eu2O3-TeO2 glasses, J. Non-Cryst. Solids 505 (2019) 400–405.
[17] N. Ghribi, M. Dutreilh-Colas, J.R. Duclère, T. Hayakawa, J. Carreaud, R. Karray, A. Kabadou, P. Thomas, Thermal, optical and structural properties of glasses within the TeO2-TiO2-ZnO system, J. Alloy. Comp. 622 (2015) 333–340.
[18] M.I. Sayyed, Bismuth modified shielding properties of zinc boro-tellurite glasses, J. Alloy. Comp. 688 (2016) 111–117.
[19] N. Elkhoshkhany, Rafik Abbas, R. El-Mallawany, S.F. Hathot, Optical properties and crystallization of bismuth boro-tellurite glasses, J. Non-Cryst. Solids 476 (2017) 15–24.
[20] Helena Ticha, Jiri Schwarz, Ladislav Tichy, The structural arrangement and the optical band gap in certain Quaternary PbO–ZnO–TeO2–B2O3 glasses, J. Non-Cryst. Solids 489 (2018) 40–44.
[21] M. Mansur Tufekci, Ahmet Gokce, Development of heavyweight high performance fiber reinforced cementitious composites (HPFRCC) – Part II: X-ray and gamma radiation shielding properties, Constr. Build. Mater. 163 (2018) 326–336.
[22] L. Gerward, N. Guilbert, K.B. Jensen, H. Levring, WinXCom - a program for calculating X-ray attenuation coefficients, Radiat. Phys. Chem. 71 (3–4) (2004) 653–654.
[23] S. Agostinelli, J. Allison, K.a. Amako, J. Apostolakis, H. Araujo, P. Arce, M. Asai, D. Axen, S. Banerjee, G. Barrand, et al., Geant4a simulation toolkit, Nucl. Instrum. Methods Phys. Res. Sect. A Accel. Spectrom. Detect. Assoc. Equip. 506 (2003) 250–303.
[24] F. Akman, M.R. Kaçal, M.I. Sayyed, H.A. Karatas, Study of gamma radiation attenuation properties of some selected ternary alloys, J. Alloy. Comp. 782 (2019)

315–322.
[25] M.I. Sayyed, F. Akman, A. Kumar, M.R. Kacal, Evaluation of radioprotection properties of some selected ceramic samples, Res. Phys. 11 (2018) 1100–1104.
[26] R. Bagheri, A. Khorrami Moghaddam, H. Yousefnia, Gamma ray shielding study of bariumebismutheborosilicate glasses as transparent shielding materials using MCNP-4C code, XCOM program, and available experimental data, Nucl. Eng. Technol. 49 (2017) 216–223.
[27] D5, S.A. Tijani, Salahuddin M. Kamal, Y. Al-Hadeethi, Mehenna Arib, M.A. Hussein, S. Wageh, L.A. Dim, Radiation shielding properties of transparent erbium zinc tellurite glass system determined at medical diagnostic energies, J. Alloy. Comp. 741 (2018) 293–299.
[28] Parminder Kaur, K.J. Singh, Sonika Thakur, Prabhjot Singh, B.S. Bajwa, Investigation of bismuth borate glass system modified with barium for structural and gamma-ray shielding properties, Spectrochim. Acta A Mol. Biomol. Spectrosc. 206 (2019) 367–377.
[29] K.J. Singh, N. Singh, R.S. Kaundal, K. Singh, Gamma-ray shielding and structural properties of PbO–SiO2 glasses, Nucl. Instrum. Methods Phys. Res. B 266 (2008) 944–948.
[30] O. Agar, M.I. Sayyed, H.O. Tekin, Kawa M. Kaky, S.O. Baki, I. Kityk, An investigation on shielding properties of BaO, MoO3 and P2O5 based glasses using MCNPX code, Res. Phys. 12 (2019) 629–634 2019.
[31] A.E. Ersundu, M. Büyükyıldız, M. Çelikbilek Ersundu, E. Şakar, M. Kurudire, The heavy metal oxide glasses within the WO3-MoO3-TeO2 system to investigate the shielding properties of radiation applications, Prog. Nucl. Energy 104 (2018) 280–287.
[32] Parminder Kaur, K.J. Singh, Sonika Thakur, Prabhjot Singh, B.S. Bajwa, Investigation of bismuth borate glass system modified with barium for structural and gamma-ray shielding properties, Spectrochim. Acta A Mol. Biomol. Spectrosc. 206 (2019) 367–377.
[33] Muhammad Khairi Azri Roslan, Mohammad Ismail, Ahmad Beng Hong Kueh, Muhammad Rawi Mohamed Zin, High-density concrete: exploring Ferro boron effects in neutron and gamma radiation shielding, Constr. Build. Mater. 215 (2019) 718–725.
[34] I.I. Bashter, Calculation of radiation attenuation coefficients for shielding concretes, Ann. Nucl. Energy 24 (1997) 1389–1401.